Supramolecular Modification of Ion Chemistry: Modulation of Peptide Charge State and Dissociation Behavior through Complexation with Cucurbit[*n*]uril (*n* = 5, 6) or α-Cyclodextrin

Haizhen Zhang,[†] Megan Grabenauer,[‡] Michael T. Bowers,[‡] and David V. Dearden*[,†]

Department of Chemistry and Biochemistry, Brigham Young University, Provo, Utah 84602-5700, and Department of Chemistry and Biochemistry, University of California, Santa Barbara, California 93106

Received: September 29, 2008; Revised Manuscript Received: January 10, 2009

Electrospray Fourier transform ion cyclotron resonance mass spectrometry, ion mobility spectrometry, and computational methods were utilized to characterize the complexes between lysine or pentalysine with three prototypical host molecules: α-cyclodextrin (α-CD), cucurbit[5]uril (CB[5]), and cucurbit[6]uril (CB[6]). Ion mobility measurements show lysine forms externally bound, singly charged complexes with either α-CD or CB[5], but a doubly charged complex with the lysine side chain threaded through the host cavity of CB[6]. These structural differences result in distinct dissociation behaviors in collision-induced dissociation (CID) experiments: the α-CD complex dissociates via the simple loss of intact lysine, whereas the CB[5] complex dissociates to yield $[CB[5] + H_3O]^+$, and the CB[6] complex loses neutral NH_3 and CO, the product ion remaining a doubly charged complex. These results are consistent with B3LYP/6−31G* binding energies (kJ mol^{-1}) of D(Lys + H^+−α−CD) = 281, D(Lys + H^+−CB[5]) = 327, and D(Lys + $2H^{2+}$−CB[6]) = 600. B3LYP/6−31G* geometry optimizations show complexation with α-CD stabilizes the salt bridge form of protonated lysine, whereas complexation with CB[6] stabilizes doubly protonated lysine. Complexation of the larger polypeptide pentalysine with α-CD forms a nonspecific adduct: no modification of the pentalysine charge state distribution is observed, and dissociation occurs via the simple loss of α-CD. Complexation of pentalysine with the cucurbiturils is more specific: the observed charge state distribution shifts higher on complexation, and fragmentation patterns are significantly altered relative to uncomplexed pentalysine: C-terminal fragment ions appear that are consistent with charge stabilization by the cucurbiturils, and the cucurbiturils are retained on the fragment ions. Molecular mechanics calculations suggest CB[5] binds to two protonated sites on pentalysine without threading onto the peptide and that CB[6] binds two adjacent protonated sites via threading onto the peptide.

1. Introduction

Studies of host−guest interactions often give fundamental insights into supramolecular chemistry.[1,2] Cyclodextrins (CDs)[3,4] and cucurbiturils (CBs)[5−7] are both important host molecules that have been extensively studied and characterized in condensed media. The simpler environment of the gas phase provides a unique opportunity to compare and contrast these important hosts without the perturbing influence of solvation and to apply high-level computational methods to gain additional insights into the fundamental factors that influence their binding properties and to compare them with the experimental findings.

Cyclodextrins are cyclic sugars with a torus-like shape. The most common CDs are α, β, and γ-CD, which are composed of 6, 7, and 8 glucose units, respectively. The interior cavity of CD is relatively hydrophobic; therefore, CD hosts can form inclusion complexes with appropriately sized molecular guests.

Cucurbiturils are pumpkin-shaped cyclic polymers of glycoluril with hollow interior cavities. Carbonyl oxygen atoms line the portals and form binding sites for positive ions, while the interior cavities are again relatively hydrophobic and can host neutral molecules that fit within. Cucurbiturils with cavities of varying sizes have been synthesized, ranging from CB[5], composed of five glycoluril units, up to CB[10], built from 10 glycolurils. The most well-known cucurbituril is CB[6], which was originally synthesized over 100 years ago and extensively characterized during the latter half of the 20th century. Figure 1 compares the structures of α-CD (a) and CB[6] (b).

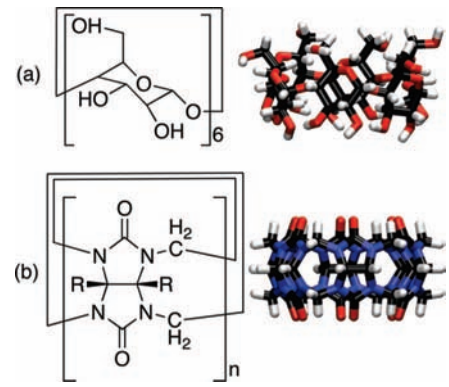

Figure 1. Structures of α-cyclodextrin (α-CD, a) and cucurbit[n]uril (CB[n], b). CB[6] is depicted in the model.

Although the sizes and shapes of these two hosts are similar, their structural differences lead to distinct binding differences. CB[6] has a symmetric geometry with two identical openings that are lined with electronegative carbonyl groups. However,

* To whom correspondence should be addressed. Department of Chemistry and Biochemistry, C100 Benson Science Building, Brigham Young University, Provo, UT 84602-5700. E-mail: david_dearden@byu.edu.
[†] Brigham Young University.
[‡] University of California, Santa Barbara.

10.1021/jp808625v CCC: $40.75
Published on Web 02/03/2009

α-CD has a less symmetric geometry with one opening to the interior lined with primary hydroxyl groups and the other lined with secondary hydroxyls. The carbonyls of CB[6] act as electronegative sites favorable for binding positive ions; they are also good hydrogen bond receptors. The hydroxyl groups that line the α-CD portals can also bind cations, but function both as hydrogen bond donors and as acceptors. Further, the α-CD scaffold is much more flexible than that of CB[6], particularly on the side that consists of primary hydroxyl groups.

Because of their ability to encapsulate smaller molecules, both cyclodextrins[8−12] and cucurbiturils[13−17] have been suggested as potential drug delivery agents, and cyclodextrins are already in wide use. The drug delivery applications of cucurbiturils are much less well developed, as water-soluble cucurbiturils have only recently been synthesized.[14,18,19] In light of these biological applications, a fundamental understanding of the interactions between these supramolecular hosts and biomolecules is important. This article represents one of the first attempts to characterize complexation between cucurbit[6]uril and amino acids or small peptides.

Mass spectrometry has been widely used to investigate host−guest interactions in the gas phase.[20−25] In addition to the fact that only miniscule sample sizes are required for extensive mass spectrometric characterization, a particular advantage of gas phase host−guest research is that the experimental results can be directly compared to computational results[25,26] because complicating interferences from solvents are not present. Thus, mass spectrometry coupled with high-level computational methods becomes a powerful tool to elucidate binding behavior in host−guest complexes. Further, concentrations on the order of micromolar are sufficient for electrospray experiments; therefore, even species with relatively low solubilities such as CB[6] can be investigated.

Supramolecular complexation also offers new opportunities for mass spectrometric characterization because complexation can influence the chemistry of gas phase ions in interesting and potentially useful ways. Prior studies of the effects of supramolecular complexation on ion chemistry include the pioneering work of Julian and Beauchamp,[27] who examined interactions of polylysines and small proteins with the crown ether 18-crown-6. They found that complexation with 18-crown-6 resulted in a shift of the observed charge states toward higher charge and an improvement in the mass spectrometric signal-to-noise over what is observed when the crown is not present. Subsequently, Julian has used the extent of crown ether complexation as a probe of protein conformation.[28] In this article, we show that such effects are sensitive to the type of complexing agent used: CB[5] and CB[6] produce results similar to those previously observed for 18-crown-6, whereas α-CD, which will be shown to bind nonspecifically, does not. Further, we will show that even the specifically binding cucurbiturils exhibit differences arising from different binding motifs.

Herein we examine the effects of supramolecular complexation on the behavior of amino acid and small peptide ions in the gas phase. Specifically, we use both quantum computational methods and mass spectrometry/ion mobility experiments to compare the effects of a set of complexing agents that differ in size and structure: CB[5], CB[6], and α-CD. We will show that these agents can be used to modify both the distribution of observed charge states and the dissociation behavior of the analytes.

All naturally occurring amino acids favor a nonzwitterionic structure in the gas phase.[29−31] This contrasts with their chemistry in solution at neutral pH, where the zwitterion form is the most stable. Lebrilla et al. demonstrated that β-CD can form inclusion complexes with amino acids[32,33] and presented evidence that the interaction between the amino acid and the narrow (primary) rim of β-CD stabilizes salt bridge formation.[34] Consequently, β-CD presents a solvent-like environment to an included amino acid. However, α-CD has a smaller cavity and portal size. On the basis of size alone, we would expect complexes between amino acids and α-CD to be different from those with β-CD. In this article, we report experiments and theory to investigate these differences and show that the surface of α-CD is sufficiently solvent-like to influence the structure of nonspecifically bound lysine.

In previous work, Dearden and co-workers characterized the pseudorotaxane structure of CB[6]-diammonium complexes in the gas phase.[35] In those pseudorotaxane complexes, linear alkyldiammonium ions are threaded through CB[6], and hydrogen bonds between the ammonium groups and the carbonyl laden portals of CB[6] hold the complex together. With amino groups at both ends of an alkyl chain, lysine is structurally similar to the alkyldiammonium species previously studied and therefore might also be expected to form a pseudorotaxane with CB[6]. Herein we report our investigations into possible pseudorotaxane formation with lysine and pentalysine.

2. Experimental Section

2.1. Materials. Cucurbit[5]uril, cucurbit[6]uril, α-cyclodextrin, L-lysine, and pentalysine were purchased from Sigma Chemical Co. (St. Louis, MO) and used without further purification.

2.2. Sample Preparation. CB[6] stock solution (1.8 mg/mL) was prepared by dissolving the solid sample in 88% formic acid (Fisher Scientific, Fair Lawn, NJ); all other stock solutions were prepared by dissolving samples in HPLC grade water (Mallinckrodt Baker Inc., Phillipsburg, NJ). Electrospray solutions were prepared by mixing CB[*n*] or α-CD with peptide solutions or diluting directly from the stock solutions. Final electrospray solutions contained equimolar analytes (10^{-4} M) with 50:50 water/methanol solvent. All of the solutions also contained 4.4% formic acid following final dilution.

2.3. ESI Mass Spectrometry. Mass spectrometric measurements at BYU were carried out using a Bruker model APEX 47e FT-ICR mass spectrometer controlled by a MIDAS data system[36] and equipped with a microelectrospray source modified from an Analytica design, with a heated metal capillary drying tube based on the design of Eyler.[37] The source was typically operated at a flow rate of 10 μL h^{-1}. To avoid possible influences of tuning on the observed analyte charge states, we collected mass spectra for charge state comparison within a short period without changing any tuning parameters. All of the mass spectra reported are averages of 10 scans for each experiment.

2.4. SORI-CID Experiments. Stored waveform inverse Fourier transform (SWIFT)[38] techniques were used to isolate target peaks on the BYU FT-ICR instrument. Sustained off-resonance irradiation collision-induced dissociation (SORI-CID)[39] experiments were performed by irradiating 1 kHz below the resonant frequency of the ion of interest. Collision gas (air) was introduced using a Freiser-type pulsed leak valve.[40] SORI events involved pulsing the background pressure in the trapping cell up to 10^{-5} mbar and applying the off-resonance irradiation for 5 s, followed by a 10 s delay to allow the trapping cell to return to baseline pressure (about 10^{-8} mbar) prior to detection. The amplitude of the SORI RF pulse was varied through a range of values from less than the threshold for dissociation to several times the threshold value. Ten scans were averaged for each SORI amplitude.

2.5. Reactivity Experiments. Neutral *n*-propylamine was introduced into the trapping cell using a controlled variable leak valve to a constant pressure ($\sim 10^{-7}$ mbar). The reaction time (between SWIFT isolation of the ionic reactant and detection of reactants and products) was varied programmatically. Data analysis was performed with a modified version of the MIDAS Analysis software that was capable of extracting peak amplitudes from a set of spectra that differ in one or more experimental parameters (in this case, reaction time).

2.6. Ion Mobility Experiments. Ion mobility experiments were performed at UCSB on a home-built instrument consisting of a nanoelectrospray ionization (nano-ESI) source, an ion funnel, a drift cell, and a quadrupole mass filter. The details and typical operating parameters of the instrument have previously been published;[41] therefore, only a brief description will be given here. In the ion mobility experiments,[42−45] ions are generated in the source from approximately 5 μL of sample solution contained in a metal coated borosilicate capillary (Proxeon, Odense, Denmark), enter the ion funnel through a 0.01 in. ID capillary, are transmitted to the mobility cell, stored, and then pulse injected at low energy into the mobility cell, which is filled with around 4 mbar of He gas. The ions are rapidly thermalized by collisions with the He gas as they travel through the cell under the influence of a weak dc electric field, E. The ions drift through the cell with a constant drift velocity, v_D, proportional to the electric field.

$$v_D = KE \tag{1}$$

The proportionality constant, K, is the ion mobility. By measuring the arrival time at the detector for several values of the field E, an accurate value of K is determined. Through the use of kinetic theory,[46] the collision cross-section σ can be obtained from the experimental value of K. Ions exiting the drift cell are collected as a function of time, yielding an arrival time distribution (ATD). Compact ions with small cross-sections drift faster and have shorter arrival times than more extended ions with larger cross-sections. Thus, different conformers can be separated in the drift cell and appear as separate peaks in the ATD. The cross-section for each conformer can be obtained as described above and their relative abundances obtained from the ATDs.

Atomic level conformational information for the complexes was obtained by comparing the experimental collision cross-sections to calculated values from molecular models. A simulated annealing protocol using the AMBER 7 package of molecular dynamics (MD) software[47] was used to generate 150−200 low energy candidate structures for each of several possible initial structures of the complex. In this protocol, an initial structure was subjected to 30 ps of molecular dynamics at 600 K followed by 10 ps of dynamics during which the temperature was lowered to 0 K. The resulting structure was then energy minimized, saved, and used as the starting structure for the next cycle. The collision cross-sections of these candidate structures were then calculated using an angle averaged projection model.[48] A scatter plot of cross-section versus energy is assembled and the lowest 3−5 kcal/mol structures used to obtain an average cross-section. Examples of the scatter plots are given in Supporting Information.

2.7. Electronic Structure Calculations. Structures were sketched using the Maestro/Macromodel modeling package (Macromodel version 7.1; Schrödinger, Inc.; Portland, OR). Conformational searches were performed using the MMFF94s[49] force field with no nonbonded cutoffs and with conjugate gradient minimization using the MCMM search method with automatic setup and 50,000 starting structures. Torsional rotations within the cucurbituril ring or within the α-cyclodextrin ring were disabled. The lowest-energy structures found in the conformational searches were used as the starting point for B3LYP/6−31G* DFT geometry optimizations. These calculations were performed using NWChem (version 4.7; Pacific Northwest National Laboratory; Richland, WA)[50] and used NWChem default convergence criteria. No atoms were constrained in the geometry optimizations; thus, if proton transfer is energetically favorable, the geometry optimization algorithm of NWChem will carry out the transfer. Computed structures were visualized using the VMD software package (version 1.8.5).[51] Reported energies are at 0 K, uncorrected for zero point energy; vibrational calculations were not carried out because for systems of the size studied here they require greater computational resources than were available to us. Because our conclusions rely on relative energies for the various complexes, and because zero point energies are expected to be similar for complexes of similar size, we do not expect large errors arising from zero point corrections.

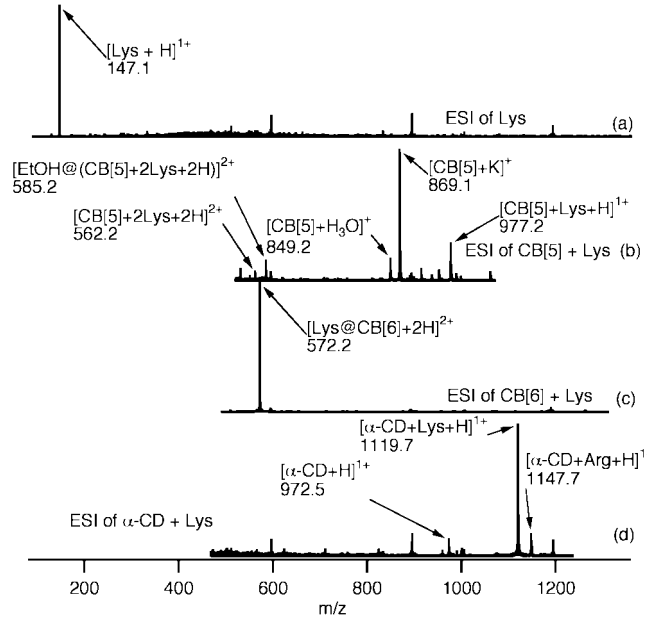

Figure 2. Mass spectra of (a) isolated lysine, (b) lysine + CB[5], (c) lysine + CB[6], and (d) lysine + α-CD. (The peak assigned to arginine+α-CD is from sample cross-contamination.)

3. Results

3.1. Lysine Complexation with CB[5], CB[6], and α-CD. ***3.1.1. Electrospray of Lysine, Lysine + CB[5], Lysine + CB[6], and Lysine + α-CD Solutions.*** Lysine, lysine + CB[5], lysine + CB[6], and lysine + α-CD solutions were each electrosprayed into the FTICR mass spectrometer (Figure 2). Sprayed alone, lysine yields a protonated +1 ion. The lysine + CB[5] ESI spectrum is the most complex, partially because the CB[5] samples contained potassium salt impurities. Although the peak may arise from fragmentation of Lys complexes in the ion source, experimental observation of [CB[5] + H_3O^+] is significant, as H_3O^+ has been proposed as a template ion in the formation of CB[5],[52] and observation of the H_3O^+ complex demonstrates that such a complex can form. Both CB[5] and α-CD form singly charged 1:1 complexes with lysine, while CB[6] forms only a doubly charged lysine adduct. All spectra were sufficiently well mass resolved that significant populations of doubly charged dimers (with the same nominal *m/z* as singly

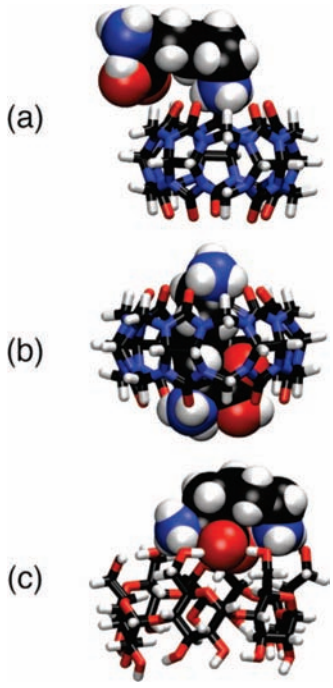

Figure 3. Lowest energy computed structures for complexes of lysine (space filling) with host species (tubes) CB[5], CB[6], and α-CD. (a) Side chain protonated, singly charged lysine externally binds to CB[5]. (b) The side chain of lysine threads through the CB[6] cavity to form a pseudorotaxane complex with both amine groups (as well as the carboxyl) protonated. (c) Protonated lysine (in salt bridge form) externally attaches to the primary hydroxyl, narrower rim of α-CD.

charged monomeric complexes) would easily be observed via their isotopic peaks. However, no evidence of such species was apparent in the FTICR mass spectra.

3.1.2. Computational Results. The lowest energy conformations found in our computational study have singly charged lysine (protonated on its side chain) bound externally on CB[5], doubly charged lysine (protonated at the termini and on its side chain) threaded through the cavity of CB[6], and singly charged lysine (protonated on its side chain and N-terminus, and deprotonated on its C-terminus (i.e., in salt bridge form)) bound externally on the primary rim of α-CD (Figure 3). For CB[5] (part a of Figure 3), lysine externally binds to the cucurbituril, the protonated lysine side chain hydrogen bonding to the electronegative portal of CB[5]; steric constraints prevent the side chain from threading into the cavity. In the CB[6] complex (part b of Figure 3), which was modeled with a +2 charge to be consistent with the ESI-FTICR results, lysine protonated at both N-terminal and side chain amino sites is threaded through the cucurbituril. This complex is held together by hydrogen bonds between the ammonium groups and the electronegative oxygen atoms that line the portals of CB[6]. In contrast, the lowest energy structure found for the singly charged α-CD complex (part c of Figure 3) is with a salt bridge lysine structure. In the singly charged α-CD complex, both protonated amino groups and the deprotonated carboxylate group form hydrogen bonds with the primary hydroxyl groups of the cyclodextrin.

Relative energies and lysine ion binding energies for the lowest-energy external and threaded structures found for the lysine complexes of CB[5], CB[6], and α-CD are given in Table 1. For CB[5], the externally bound lysine structure lies more than 230 kJ mol^{-1} lower in energy than the lowest-energy threaded structure found in our conformational search. Placement of protonated lysine within the CB[5] cavity both introduces steric strain into the system and constrains placement of the lysine to a less than optimal position for hydrogen bonding with the CB[5] carbonyl oxygen atoms.

For CB[6], the threaded structure is far lower in energy (by more than 660 kJ mol^{-1}) than the externally bound structure; in fact, the latter lies higher in energy than separated and relaxed CB[6] + $(Lys + 2H)^{2+}$. For the threaded structure, the computed binding energy of doubly protonated lysine is 600 kJ mol^{-1}. For α-CD, the externally bound lysine complex lies at far lower energy than the lowest-energy threaded structure located in our searches (by almost 650 kJ mol^{-1}); the internally bound structure lies higher in energy than the separated and relaxed α-CD + $(Lys + H)^{+}$.

3.1.3. Ion Mobility Experiments. The mass spectra and arrival time distributions for the three systems taken on the UCSB instrument are given in Figure 4. These mass spectra differ somewhat from those given in Figure 2 (taken on the BYU FT-ICR), probably because the instruments are very different. The primary difference is observation of dimers on the UCSB instrument (discussed later). Both mass spectra yield 1:1 complexes, however, which is the primary focus of this work. The ATDs for the 1:1 complexes with lysine are shown as inserts in Figure 4. For $[CB[5] + Lys + H]^{+}$, the ATD has only a single peak corresponding to a cross-section of 184 $Å^2$. Similarly, the ATD for $[CB[6] + Lys + 2H]^{2+}$ is also a single peak with cross-section of 189 $Å^2$. However, the ATD for [α-CD + Lys + $H]^{+}$ is clearly bimodal with peaks at 620 and 770 μs. In all experiments, an injection energy needs to be applied to transfer the ions from the low pressure ion funnel to the higher pressure mobility cell. Normal injection energies are 40 to 50 eV with a range of ~20 to >100 eV. When complex ATDs are observed, varying the injection energy helps assign the various features.[53] At low injection energies the complexes are only minimally collisionally excited on entering the mobility cell, but at high injection energies, sufficient internal energy can be imparted to either structurally isomerize a species or dissociate an aggregate, or both. Injection energy studies indicate that the short time feature (620 μs) disappears as energy increases, eventually leaving only the feature at 770 μs (see data in Supporting Information). These results are consistent with the 770 μs feature being the [α-CD + Lys + $H]^{+}$ monomer and the 620 μs feature the $[\alpha\text{-CD} + Lys + H]_2^{2+}$ dimer.

The experimental cross-sections and possible structural assignments are gathered in Table 2. For $[CB[5] + Lys + H]^{+}$, there is good correspondence between the experimental cross-section and an externally bound protonated lysine. For $[CB[6] + Lys + 2H]^{2+}$, the experimental cross-section agrees well with a threaded doubly protonated lysine, whereas the externally bound lysine yields a cross-section much larger than the experimental one. Both of these results agree nicely with the predicted lowest energy structures of DFT calculations.

The α-CD results are not as clear-cut. The shorter time peak at 620 μs that disappears at high injection energies has a cross-section much too small for any possible monomer structure. This result is consistent with it being due to a doubly charged dimer (and consequently twice the cross-section).[53] The ATD peak at 770 μs yields a cross-section in good agreement with the model cross-sections supporting its assignment to [α-CD + Lys + $H]^{+}$, although the results are consistent with the lysine attached to either rim of α-CD and having either a salt bridge or charge solvation structure. To help resolve this dilemma, binding energies were calculated using AMBER for the two forms, indicating that the salt bridge form is bound about 70 kJ/mol stronger than the charge solvation form and that it was bound ~12 kJ/mol stronger to the wider rim (secondary OH

TABLE 1: Computational Comparison of External and Threaded Lysine (Lys) Complexes of Cucurbit[5]uril (CB[5]), Cucurbit[6]uril (CB[6]), and α-Cyclodextrin (α-CD)

complex	Lys protonation	relative energy (kJ mol^{-1})	D[(Lys+nH)$^{n+}$ − Host] (kJ mol^{-1})
[CB[5] + Lys + H]$^{1+}$ (external)	side chain	0	327
[Lys@CB[5] + H]$^{1+}$ (threaded)	side chain	233	150
[CB[6] + Lys + 2H]$^{2+}$ (external)	side chain, N-terminus, C-terminus	661	not bound
[Lys@CB[6] + 2H]$^{2+}$ (threaded)	side chain, N-terminus, C-terminus	0	600
[α-CD + Lys + H]$^{1+}$ (external)	salt bridge	0	281
[Lys@α-CD + H]$^{1+}$ (threaded)	salt bridge	647	not bound

groups) than to the narrow rim (primary OH groups). The MMFF conformational search found no conformations with the salt bridge form bound to the secondary rim within 50 kJ/mol of the lowest energy structure, which was bound on the primary rim. At the B3LYP/6−31G* level of theory, the differences

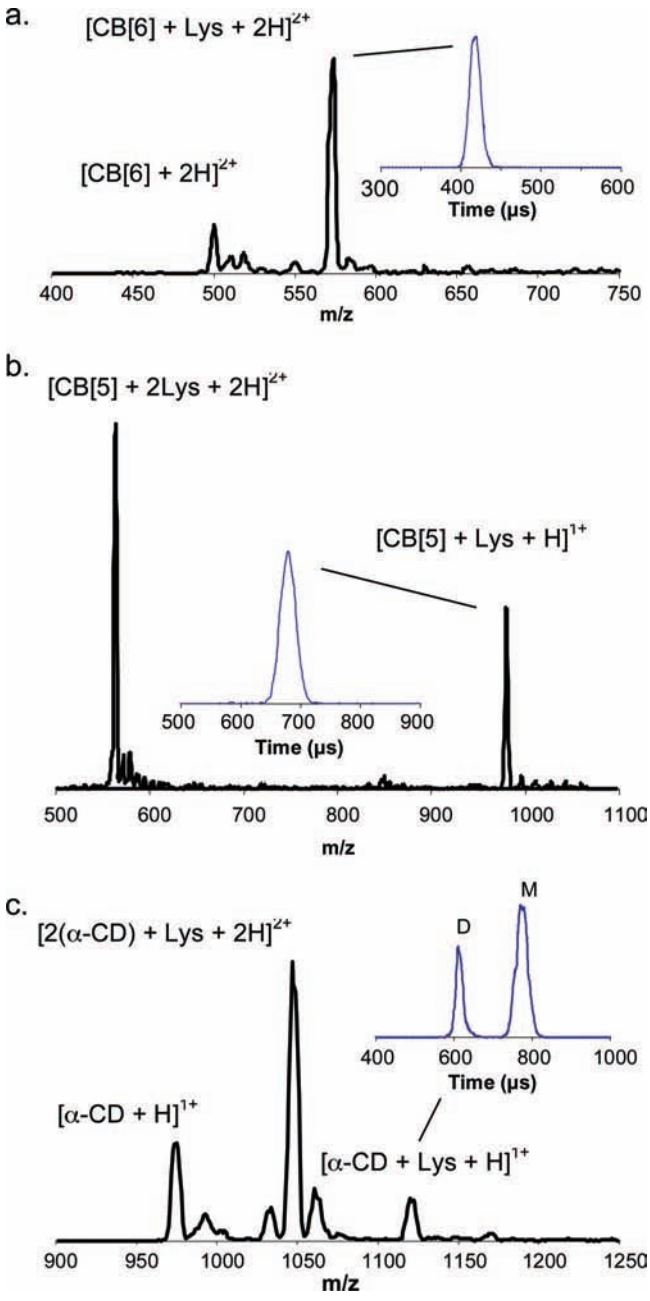

Figure 4. Mass spectra taken on the UCSB instrument. The insets are arrival time distributions of the designated peaks: (a) lysine + CB[6]; (b) lysine + CB[5]; (c) lysine + α-cyclodextrin.

TABLE 2: Experimental and Theoretical Model Cross-Sections

	Theory		Experiment	
	Model	Cross Section (Å^2)	Time (μs)[c]	Cross Section (Å^2)
CB[5] + Lys[a]		170 (SB)[d] 170 (CS)	690	184
		186 (SB)[d] 187 (CS)		
CB[6] + Lys[b]		193	420	189
		218-225		
α-CD + Lys[b]		217 (SB)[d] 220 (CS)	620	M[e] (155) D[e] (312)
		224 (SB)[d] 218 (CS)	770	220

[a] Single protonated lysine. [b] Doubly protonated lysine. [c] From ATD insets in Figure 4. [d] SB = salt bridge; CS = charge solvation. [e] M = monomer; *D* = dimer.

are smaller but show the same trends with regard to the salt bridge and charge solvation forms: the salt bridge form is bound 9 kJ/mol stronger than the charge solvation form (protonated at the N-terminus; the side chain protonated form has essentially the same energy). Binding on the secondary rim was not examined at this level of theory because the MMFF search provided no starting structures bound on the secondary rim. The experimental cross-section (220 Å^2) is slightly smaller than the salt bridge ligated model cross-section (224 Å^2). This small difference is consistent with the fact the experimental cross-sections for the CB[5] and CB[6] complexes are also slightly smaller than the model cross-sections.

The mass spectra taken on the UCSB instrument (Figure 4) differ from the BYU FT-ICR spectra. The primary differences are for the CB[5] and α-CD systems (parts b and c of Figure 4) where the largest features observed are [CB[5] + 2Lys + 2H]$^{2+}$ and [2α-CD + Lys + 2H]$^{2+}$. The relative intensity of the [CB[5] + 2Lys + 2H]$^{2+}$ peak is much lower in the FTMS spectrum in part b of Figure 2, and the [2α-CD + Lys + 2H]$^{2+}$ peak is not evident in part d of Figure 2. The different results are almost certainly due to the very different source conditions in the two experiments since identical solutions were used on both instruments. The explanation for the differences may be that the

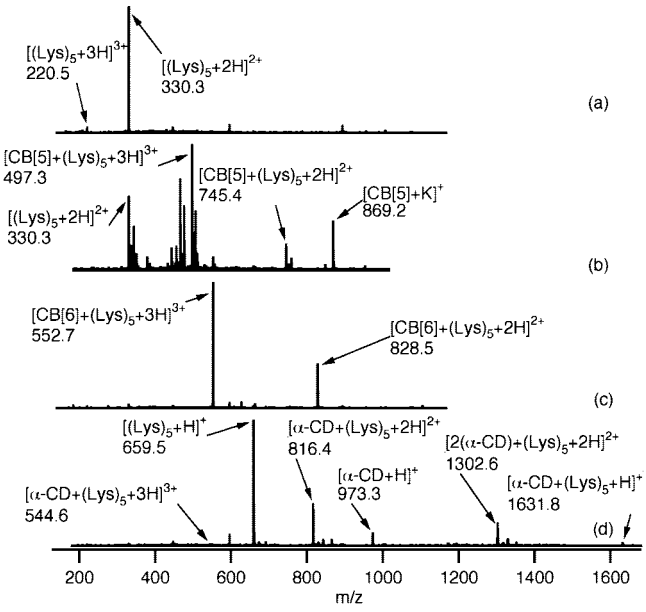

Figure 5. ESI spectra of (a) pentalysine, (b) pentalysine + CB[5], (c) pentalysine + CB[6], and (d) pentalysine + α-CD.

source conditions are relatively harsh on the BYU FTICR, leading to dissociation of these relatively weakly bound complexes on that instrument. This explanation would also be consistent with the fact that the $[\alpha\text{-CD} + \text{Lys} + \text{H}]_2^{2+}$ dimer is not observed on the BYU FTICR.

3.1.4. SORI-CID of Lysine and Its Complexes. Under collisional activation, the singly charged lysine ion dissociates by losing ammonia, water, and carbon monoxide. However, complexation alters the SORI-CID spectrum: the singly charged lysine-CB[5] complex yields only one observed ionic fragment, an ion corresponding to $[\text{CB}[5] + \text{H}_3\text{O}]^+$. Similarly, activation of $[\text{CB}[6] + \text{Lys} + 2\text{H}]^{2+}$ yields only one fragment ion, a doubly charged ion corresponding to loss of water and carbon monoxide. In contrast, the singly charged lysine-α-CD complex dissociates without breaking covalent bonds, via the loss of either neutral lysine or loss of neutral α-CD. Data are presented in Supporting Information.

3.2. Pentalysine Complexation. Pentalysine includes the same functional groups as lysine but has three times as many basic sites (six). With more basic sites, under acidic spray conditions it is possible to achieve higher charge states than can be observed for lysine alone. Further, with this larger peptide additional binding motifs are possible. To probe the greater complexity afforded by pentalysine, we examined its complexes with CB[5], CB[6], and α-CD.

3.2.1. ESI Mass Spectra of Pentalysine and Its Complexes. ESI-FTICR/MS spectra of pentalysine and its complexes with CB[5], CB[6], and α-CD are given in Figure 5. Sprayed alone, the dominant charge state for pentalysine is +2, with the +3 charge state being only a few percent as intense. Addition of cucurbituril yields complexes with enhanced abundance of higher charge states. For both CB[5] and CB[6], the $[\text{CB}[n] + (\text{Lys})_5 + 3\text{H}]^{3+}$ peak is more intense than that corresponding to $[\text{CB}[n] + (\text{Lys})_5 + 2\text{H}]^{2+}$. The CB[5] spectrum is significantly contaminated with K^+ adducts, and the peak for unreacted $[(\text{Lys})_5 + 2\text{H}]^{2+}$ is more than 50% as intense as the base peak, $[\text{CB}[5] + (\text{Lys})_5 + 3\text{H}]^{3+}$. Addition of CB[6] results in simpler spectra, the only prominent peaks being the triply and doubly protonated complexes of pentalysine with CB[6]. For the α-CD mixture, uncomplexed, singly protonated pentalysine is the major peak along with a prominent signal corresponding to $[\alpha\text{-CD} + (\text{Lys})_5 + 2\text{H}]^{2+}$. An additional interesting peak is observed at m/z 1302.6, corresponding to $[2\alpha\text{-CD} + (\text{Lys})_5 + 2\text{H}]^{2+}$. Similarly, two α-CD molecules can also attach to one doubly protonated lysine molecule (part b of Figure 4).

3.2.2. SORI of Pentalysine and Its Complexes. Figure 6 shows SORI-CID spectra of the +2 charge states of pentalysine and its complexes with CB[5] and CB[6]. In the figure and in the discussion that follows, peptide fragmentation is described in terms of the nomenclature of Roepstorff.[54]

Collisional activation of uncomplexed pentalysine (part a of Figure 6) results in water losses and the complete series of b fragment ions.

Complexation with CB[5] (part b of Figure 6) yields singly charged y_1 and y_2 cleavage products with the CB[5] ligand still attached. Interestingly, simple loss of CB[5] from the peptide is not observed.

The CID spectrum of the +2 pentalysine-CB[6] complex (part c of Figure 6) is dominated by $(\text{CB}[6] + b_n)^{2+}$ and $(\text{CB}[6] + y_n)^{2+}$, $n = 2-4$ although the resolution is not sufficient to eliminate H_2O loss from $(\text{CB}[6] + y_n)^{2+}$ as a contributor to the intensity of the $(\text{CB}[6] + b_n)^{2+}$ ion signal. The small peaks 36 amu below $(\text{CB}[6] + y_n)^{2+}$ may be double water losses from $(\text{CB}[6] + y_n)^{2+}$ or single water losses from $(\text{CB}[6] + b_n)^{2+}$. Of interest is the fact that a $(\text{CB}[6] + a_1)^{1+}$ product is present, but is not found in the CID of pentalysine itself where a b_1 fragment is observed.

CID of the +3 charge state, $(\text{CB}[6] + \text{Lys}_5 + 3\text{H})^{3+}$ (Supporting Information), gives results similar to those observed for the +2 charge state, except that the relative abundance of the $(\text{CB}[6] + y_n)^{2+}$ fragments decreases, and the $(\text{CB}[6] + a_1)^{2+}$ fragment becomes the most abundant peak. No triply charged fragments were observed.

In contrast with the cucurbituril complexes, the $[\alpha\text{-CD} + (\text{Lys})_5 + 2\text{H}]^{2+}$ complex fragments via simple cleavages under SORI conditions with the principle products being $[\alpha\text{-CD} + \text{H}]^{1+}$, $[(\text{Lys})_5 + \text{H}]^{1+}$, and water losses (Supporting Information).

4. Discussion

4.1. Threaded versus Nonthreaded Structures in the Gas Phase. We recently demonstrated that threaded and nonthreaded structures involving CB[6] and 1,4-diaminobutane could be distinguished via their CID and reactivity behaviors.[35,55] The threaded complex dissociated via covalent cleavages of the host and guest, whereas the nonthreaded complex dissociated via separation of the two intact molecules. Exposure of the threaded complex to a neutral amine resulted in a slow addition of the amine to the complex, but the nonthreaded complex was much more reactive, with the added amine rapidly replacing nonthreaded 1,4-diaminobutane. Complexes of lysine with CB[5], CB[6], and α-CD can be characterized in the same way.

The data suggest that lysine binds externally to both CB[5] and α-CD in the gas phase. The SORI-CID results are clearest for the α-CD complex: $[\alpha\text{-CD} + \text{Lys} + \text{H}]^{2+}$ dissociates via simple cleavage of the noncovalent associations between the two molecules, yielding $[\text{Lys} + \text{H}]^{1+}$ and $[\alpha\text{-CD} + \text{H}]^{1+}$, consistent with external binding (Supporting Information). The interaction between Lys and CB[5] evidently is stronger because simple noncovalent cleavage products are not observed. Rather, Lys dissociates forming the $[\text{CB}[5] + \text{H}_3\text{O}]^{1+}$ complex.

Similarly, reactivity experiments suggest that lysine binds externally to both CB[5] and α-CD. For both complexes, neutral *n*-propylamine rapidly displaces lysine. The ion mobility experimental results are consistent with externally bound lysine in both cases, whereas the measured collision cross-sections are

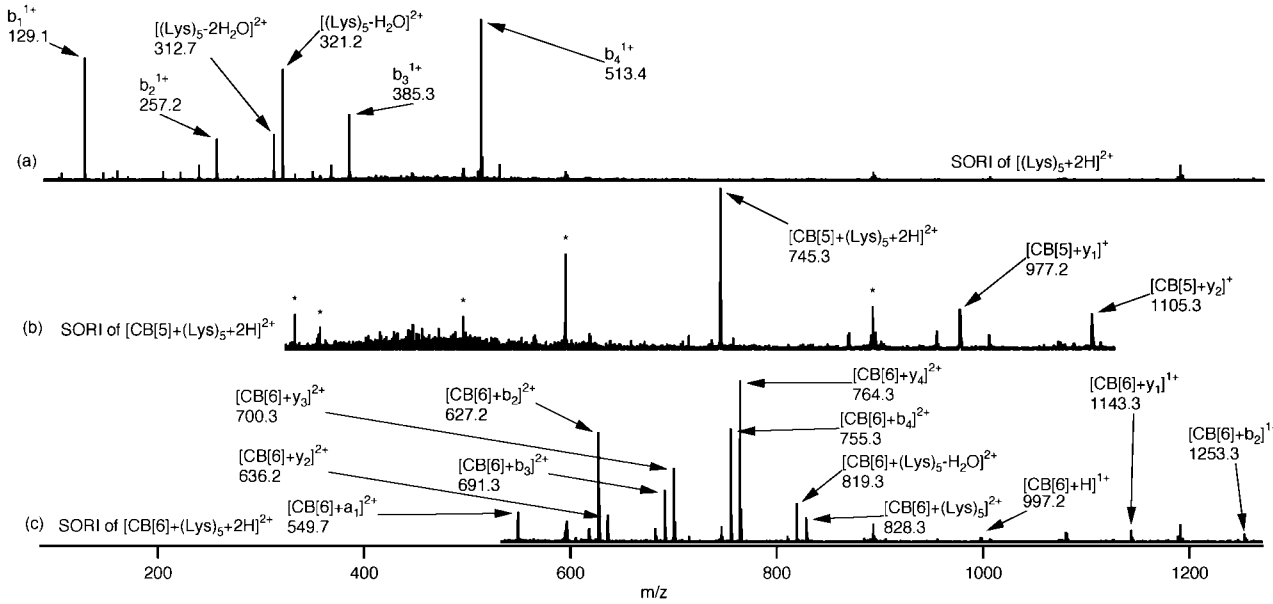

Figure 6. SORI-CID spectra of the +2 charge states of (a) pentalysine; (b) pentalysine + CB[5]; and (c) pentalysine + CB[6]. Asterisks indicate prominent noise peaks.

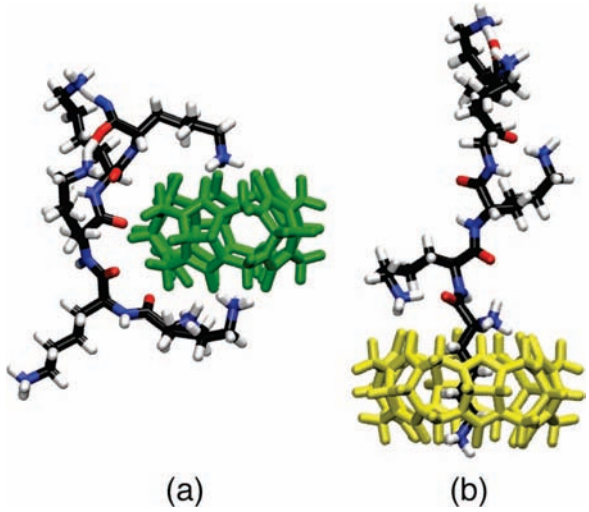

Figure 7. Low energy complexes of +5 pentalysine with CB[5] (green, a) and CB[6] (yellow, b), from Monte Carlo-MMFF conformational searching.

significantly larger than those computed for internally bound lysine. Finally, the computational results show that the externally bound structures are lower in energy than the threaded structures, by 233 and 647 kJ mol^{-1}, for the CB[5] and α-CD complexes, respectively.

The observation of [CB[5] + 2Lys + 2H]$^{2+}$ on both instruments (part b of Figure 2 and part b of Figure 4) is also noteworthy in the context of threaded versus nonthreaded structures. As both rims of the CB[5] torus are identical, and the protonated lysine binds externally, it is not surprising that both sites should be occupied. Similarly, in the ESI spectrum of pentalysine sprayed with CB[5] (part b of Figure 5), only 1:1 complexes are evident even for the multiply protonated species, consistent with the idea that one CB[5] may bind two protonation sites and with low-energy computed structures that show CB[5] pinched between two protonated side chains (vide infra, see part b of Figure 7). In contrast, doubly protonated lysine threads through the CB[6] cavity (vide infra), and only one binding site is available for threaded binding; therefore, only 1:1 complexation is observed for CB[6]. For α-CD, the two rims are not identical. It is likely that lysine preferentially binds on one of the rims; therefore, again only 1:1 complexation is observed for α-CD; when the preferred site is occupied, binding does not occur on the nonpreferred rim.

All of the available experimental and computational evidence supports a threaded structure for the complex of doubly charged lysine with CB[6]. When the complex is collisionally activated, lysine loses water and carbon monoxide, yielding a doubly charged fragment ion that remains associated with CB[6]. Thus, covalent cleavages are more favorable than simple disruption of all the ionic hydrogen bonds (as many as 6) in the complex. When the complex is exposed to *n*-propylamine, displacement of lysine does not occur; rather, the *n*-propylamine slowly adds to the complex. This is directly analogous to the previously observed reactivity of the threaded 1,4-diaminobutane complex with CB[6] and in contrast to the rapid displacement observed when that complex is not threaded.[35] The ion mobility results show close agreement between experimental and model collision cross-sections for the threaded structure, whereas the model cross-section for the structure with lysine bound externally is about 10% greater than the experimental value. Computationally, the threaded structure lies 661 kJ mol^{-1} lower in energy at the B3LYP/6−31G* level than the lowest energy externally bound structure.

4.2. Influence of Complexation on Salt Bridge Stability. It has long been known that amino acids form zwitterions in aqueous solution over a wide pH range, whereas it has more recently been shown that they exist as nonzwitterions in the gas phase.[29−31] Complexation with a large host molecule represents an intermediate state between isolation in the gas phase and full solvation. Are amino acids most stable as zwitterions when complexed? Can we control their charge distribution by controlling the complexation environment? Here, we focus on protonated lysine to attempt to address these questions.

Three sites on the lysine molecule can be protonated: the N-terminal amino group, the side chain amino group, and the carboxylate group. Singly charged (+1) lysine could therefore be protonated at either of the basic sites along with the acid group, or it could be protonated at both basic sites with a

TABLE 3: B3LYP/6−31G* Relative Energies of Gas Phase Lysine +1 Tautomers and Their Complexes (kJ mol^{-1})

host	protonation site		
	N-terminal	side chain	salt bridge
none	21	0	56
CB[5] (external)	50	0	42
CB[6] (external)	34	0	36
CB[6] (internal)	0	12	[a]
α-CD (external)	3	3	0

[a] Not a minimum.

deprotonated carboxylate. Relative energies of singly protonated gas phase lysine in various environments are given in Table 3. At the B3LYP/6−31G* level of theory for protonated lysine isolated in the gas phase, placement of the proton on the amino side chain is the lowest energy form, followed by N-terminal protonation (21 kJ mol^{-1} higher), with the salt bridge being highest in energy (56 kJ mol^{-1} above the side chain protonated form).

Lebrilla and co-workers recently demonstrated that interactions between amino acids and the primary rim of β-cyclodextrin can stabilize salt bridge formation.[34] The polar groups of the cyclodextrin present a local methanol-like environment to the amino acid, stabilizing the separation of charge in the salt bridge form. It is therefore reasonable to expect that complexes with other host molecules possessing polar substituents should have similar effects. The B3LYP/6−31G* computational results in Table 3 suggest this expectation has merit. Because of its close similarity to β-cyclodextrin, complexation with α-CD would be expected to lower the relative energy of the salt bridge form of protonated lysine. Table 3 shows that this is the case; all three tautomers of protonated lysine have very similar energies at this level of theory when bound to α-CD.

Like α-CD, the cucurbiturils also present a region of hydrogen bond acceptors at their rims. Will the cucurbiturils also stabilize the lysine salt bridge? For the externally bound lysine complexes, the computational results in Table 3 suggest the cucurbituril rims do lower the energy of the salt bridge form relative to the side chain protonated form of lysine. As the cucurbituril gets larger and the host becomes more flexible and solvent-like, the relative energy of the salt bridge form drops. The cucurbituril environment strongly destabilizes N-terminal protonation relative to side chain protonation, probably because side chain protonation is strongly stabilized by the polar cucurbituril rim.

The interior of the CB[6] cavity is a very different environment, where the salt bridge structure is destabilized to the point it is not a minimum. Insight comes from B3LYP/6−31G* geometry optimizations that began with the lysine threaded through the cavity of CB[6] but with the lysine in a salt bridge form. Despite beginning with a salt bridge structure, the proton located on the N-terminus moves to the carboxyl during energy minimization. The steric constraints imposed by the cavity force the carboxylic acid group close to the electronegative CB[6] carbonyl groups, lowering the stability of the negative carboxylate. Protonation at either of the amino sites is favorable when singly protonated lysine is bound inside CB[6], but according to the calculation, N-terminal protonation is 12 kJ mol^{-1} more favorable.

Only the doubly charged complex of lysine with CB[6] was observed via electrospray mass spectrometry. Given the functional groups of lysine, the lysine in this complex cannot be a salt bridge; the lysine must be protonated at both amino groups and at the carboxylate to have a +2 charge. Thus, the complexation environment plays a large role in the energetics of lysine protonation and can be used to control which sites are protonated.

4.3. Influence of Complexation on Collision-Induced Dissociation. Comparison of the CID spectra of lysine ion and its complexes with α-CD, CB[5], or CB[6] serves as a probe of how complexation can influence ion fragmentation in simple yet subtle ways. Collisionally activated lysine ion dissociates by losing small, stable fragments: ammonia, water, and carbon monoxide. Complexation with α-CD shuts down these pathways, which involve cleavage of covalent bonds, in favor of a new low-energy pathway involving disruption of the weak noncovalent interactions that hold the complex together.

$[Lys + CB[5] + H]^+$ represents an intermediate case. Lys is externally bound via relatively weak hydrogen bonding interactions, but cumulatively, these interactions are strong enough that covalent cleavage of Lys and formation of a stable $[CB[5] + H_3O]^+$ complex is the dominant dissociation process.

Perhaps the most interesting results are those for the doubly charged Lys-CB[6] complex. B3LYP/6−31G* geometry optimization for this complex results in a doubly protonated lysine ion threaded through the hollow cavity of CB[6], held in place by hydrogen bonding with the electronegative oxygens of the CB[6] portals to form a stable pseudorotaxane. Collectively, the six hydrogen bonds between the lysine ion and CB[6] are so strong that collisional activation breaks the covalent bonds within lysine more readily than the entropically disfavored disruption of all the hydrogen bonds to free the guest from the host. Like lysine alone, the complex dissociates by losing water and carbon monoxide, but the resulting doubly charged fragment ion remains captured inside CB[6]. Interestingly, the prominent ammonia loss pathway observed for singly charged, isolated lysine is not observed for $[Lys + CB[6] + 2H]^{2+}$. Again this is consistent with the computed structure; both amino groups of doubly charged Lys are protonated and held in place by hydrogen bonds in the complex. Loss of ammonia would disrupt this energetically favorable arrangement.

4.4. Pentalysine Complexation with CB[*n*]. Attachment of either CB[5] or CB[6] to pentalysine results in a shift in the observed charge state distribution, from a strongly dominant +2 charge state for pentalysine alone to a distribution of +2 and +3, with +3 favored, for the CB[5] and CB[6] complexes (Figure 5). This is not surprising given that the cucurbiturils have two electronegative sites suitable for binding ammonium ions.

Pentalysine has 5 side chain amino sites as well as the N-terminus; any of these sites may be protonated. Where do CB[*n*] molecules attach to this longer chain? Computationally, the most thorough way to address this question (for the +3 charge state) would be to model each of the 20 possible combinations of 3 charges attached to the various protonation sites and carry out exhaustive conformational searches for each. However, with the computational resources available to us, this would be costly. A less correct, but more straightforward (and cheaper) way to address this question is to protonate all of the possible sites and perform a conformational search in which the CB[*n*] is free to move (Figure 7). This approach will not explore conformational space as thoroughly but still gives some insight into which binding sites may be favored. The lowest energy structure found for CB[5] in such a calculation has CB[5] pinched between two protonated side chains, consistent with the idea that the CB[5] portal is too small to allow easy threading of an alkyl chain through the CB[5] cavity. The same type of

calculation for CB[6] finds the cucurbituril threaded on the N-terminal lysine residue such that the two CB[6] portals form multiple hydrogen bonds with the protonated N-terminus and the protonated amino group of the N-terminal side chain. This suggests that this N-terminal site is the preferred binding site for CB[6].

For the +2 charge state of pentalysine (Figure 6a), the observed fragmentations include loss of water and various cleavages resulting in b fragments (b_1-b_4). Interestingly, the complementary y fragments are not observed. If the C-terminus is deprotonated as it would be in a pentalysine salt bridge, it is possible that the y fragments have a net charge of zero, preventing mass spectrometric detection.

The CID products from dissociation of the +2 pentalysine-CB[5] complex (part b of Figure 6) are singly charged y_1 and y_2 fragments of the peptide, each with CB[5] remaining attached. If, as the molecular mechanics calculations suggest, CB[5] binds preferentially on protonated lysine side chains, the charge-promoting presence of CB[5] may account for the observation of the y fragments. If structures of the type shown in Figure 7 are abundant, cleavage of the peptide chain remote from the CB[5] binding site would not necessarily result in a shift in mass because both fragments could remain attached to CB[5]. SORI amplitudes that result in the complete loss of the parent ion for uncomplexed +2 pentalysine or the +2 pentalysine-CB[6] complex leave significant +2 pentalysine-CB[5] parent ion, suggesting this may occur (part b of Figure 6). Similar behavior has been demonstrated in electron capture dissociation spectra of peptides, where covalent bond rupture occurs without a change in mass because other features of the secondary structure (such as, for example, disulfide linkages) hold the fragments together; some other form of ion activation (such as collisional activation) in combination with the electron capture dissociation is required to observe fragments in such cases.[56−58]

The CID spectrum of the +2 pentalysine-CB[6] complex (part c of Figure 6) has several interesting differences from the CID spectrum of +2 pentalysine alone. First, all of the products are complexed with CB[6], providing strong evidence that any of the five side chains can bind with CB[6]. Also, in CID of the +2 complex, both b and y pentalysine fragments are observed (all bound to CB[6]), and the y fragments are quite prominent. This provides additional support for the hypothesis that binding by CB[6] destabilizes a C-terminal anion: if the C-terminus is protonated, net positive charge remains on the y fragment, and it is detected. It is also interesting that almost all of the fragments are +2 charge states (except y_1 and b_2). Again, this is consistent with the idea that the two cation binding sites of CB[6] stabilize two positive charges.

Finally, despite the fact that the b_1 fragment is prominent in the CID spectrum of +2 pentalysine, the b_1 fragment is not observed in the CID spectrum of the CB[6] complex. Instead, an a_1-CB[6] product is present. In an attempt to understand these observations, we performed B3LYP/6−31G* calculations to compare the relative stabilities of the doubly charged a_1-CB[6] and b_1-CB[6] complexes. The former minimized easily, but the complex that initially had the acylium b_1-CB[6] structure produced by simple cleavage of the peptide did not converge to a stable minimum. Rather, as the geometry optimization progressed, the b_1-CB[6] complex lost carbon monoxide, becoming an a_1-CB[6] complex, in beautiful agreement with experimental observations. This is consistent with suggestions in the literature[59] that the acylium form is not stable. Cyclization of the b_1 ion via nucleophilic attack of the side chain on the carbonyl does yield a stable b_1 ion, but this cannot happen if the side chain is threaded through CB[6]. Binding with CB[6] therefore destabilizes the b_1 fragment and stabilizes the unexpected a_1 fragment instead.

5. Conclusions

Supramolecular complexation can have dramatic effects on the mass spectrometry of amino acids and small peptides. Aside from the obvious mass shifts that occur upon complex formation, shifts in the observed charge states and large changes in collisional dissociation behavior can occur. These changes are dependent on the specific nature of the complexes. In this study, complexes of α-CD, CB[5], and CB[6] with lysine and pentalysine each exhibit distinct behaviors, which arise from nonspecific binding, specific binding without mechanical interlocking, and pseudorotaxane formation, respectively.

These observations have interesting and potentially useful implications for techniques that use complexation as a probe of protein or other large molecule conformation and structure.[28] Because the resulting mass spectra depend in easily measurable ways on the nature of the noncovalent interactions, care must be taken to account for such effects as the results of complexation-probing experiments are evaluated. However, the sensitive dependence of the results on the details of complex formation suggests that a great deal of information can likely be obtained by observing the changes that occur as the probe molecule is varied. We expect such studies to become more useful as understanding of gas phase supramolecular complexation grows.

Supramolecular complexation also offers another approach to bridging the gap between the gas phase and bulk behavior. Besides sequential addition of solvent molecules to an ion, solvent-like conditions can be provided through the addition of a suitable complexing agent. Even nonspecific complexes such as that of lysine with α-CD can be useful in this regard, and indeed, such complexes probably provide a better model of solvation than specific complexation could.

Acknowledgment. We gratefully acknowledge the support of the National Science Foundation under grants CHE-0615964 (D.V.D.) and CHE-0503728 (M.T.B.).

Supporting Information Available: Cross-section versus energy scatter plot for α-CD complex with singly charged salt bridge lysine, dependence of arrival time distribution on injection energy, SORI-CID spectra for lysine and its complexes and for pentalysine and its complexes, energies and Cartesian coordinates for computed stationary points. This material is available free of charge via the Internet at http://pubs.acs.org.

References and Notes

(1) Cram, D. J.; Cram, J. M. *Science* **1974**, *183*, 803–809.
(2) Schneider, H. J. *Angew. Chem., Int. Ed. Engl.* **1991**, *30*, 1417–1436.
(3) Bender, M. L.; Komiyama, M. *Cyclodextrin Chemistry*, Springer-Verlag: Berlin, Germany, 1978.
(4) *Cyclodextrins*; Szejtli, J., Osa, T., Eds.; Elsevier: Oxford, 1996; Vol. 3.
(5) Mock, W. L. In *Comprehensive Supramolecular Chemistry*; Vögtle, F. , Ed.; Elsevier: New York, 1996; Vol. 2, pp 477−493.
(6) Lagona, J.; Mukhopadhyay, P.; Chakrabarti, S.; Isaacs, L. *Angew. Chem., Int. Ed.* **2005**, *44*, 4844–4870.
(7) Kim, J.; Jung, I.-S.; Kim, S.-Y.; Lee, E.; Kang, J.-K.; Sakamoto, S.; Yamaguchi, K.; Kim, K. *J. Am. Chem. Soc.* **2000**, *122*, 540–541.
(8) Li, J.; Loh, X. J. *Adv. Drug Delivery Rev.* **2008**, *60*, 1000–1017.
(9) Uekama, K.; Hirayama, F.; Arima, H. *Cyclodextrins Their Complexes* **2008**, 381–422.
(10) Loftsson, T.; Duchene, D. *Int. J. Pharm.* **2007**, *329*, 1–11.
(11) Davis, M. E.; Brewster, M. E. *Nat. Rev. Drug Discovery* **2004**, *3*, 1023–1035.

(12) Szejtli, J. *Pure Appl. Chem.* **2004**, *76*, 1825–1845.
(13) Lim, Y.-B.; Kim, T.; Lee Jae, W.; Kim, S.-M.; Kim, H.-J.; Kim, K.; Park, J.-S. *Bioconjugate Chem.* **2002**, *13*, 1181–1185.
(14) Jon, S. Y.; Selvapalam, N.; Oh, D. H.; Kang, J.-K.; Kim, S.-Y.; Jeon, Y. J.; Lee, J. W.; Kim, K. *J. Am. Chem. Soc.* **2003**, *125*, 10186–10187.
(15) Lee, H.-K.; Park, K. M.; Jeon, Y. J.; Kim, D.; Oh, D. H.; Kim, H. S.; Park, C. K.; Kim, K. *J. Am. Chem. Soc.* **2005**, *127*, 5006–5007.
(16) Wheate, N. J.; Buck, D. P.; Day, A. I.; Collins, J. G. *Dalton Trans.* **2006**, 451–458.
(17) Wheate, N. J.; Taleb, R. I.; Krause-Heuer, A. M.; Cook, R. L.; Wang, S.; Higgins, V. J.; Aldrich-Wright, J. R. *Dalton Trans.* **2007**, 5055–5064.
(18) Zhao, J.; Kim, H.-J.; Oh, J.; Kim, S.-Y.; Lee, J. W.; Sakamoto, S.; Yamaguchi, K.; Kim, K. *Angew. Chem., Int. Ed.* **2001**, *40*, 4233–4235.
(19) Lee, J. W.; Samal, S.; Selvapalam, N.; Kim, H.-J.; Kim, K. *Acc. Chem. Res.* **2003**, *36*, 621–630.
(20) Vincenti, M. *J. Mass Spectrom.* **1995**, *30*, 925–939.
(21) Brodbelt, J. S.; Dearden, D. V. In *Physical Methods in Supramolecular Chemistry*; Davies, J. E. D., Ripmeester, J. A., Eds.; Pergamon: Oxford, 1996; Vol. 8, pp 567−591.
(22) Dearden, D. V. In *Physical Supramolecular Chemistry*; Echegoyen, L., Kaifer, A. E., Eds.; Kluwer: Dordrecht, The Netherlands, 1996; pp 229−247.
(23) Dearden, D. V.; Zhang, H.; Chu, I.-H.; Wong, P.; Chen, Q. *Pure Appl. Chem.* **1993**, *65*, 423–428.
(24) Vincenti, M.; Pelizzetti, E.; Dalcanale, E.; Soncini, P. *Pure Appl. Chem.* **1993**, *65*, 1507–1512.
(25) Wyttenbach, T.; Batka, J., Jr.; Gidden, J.; Bowers, M. T. *Int. J. Mass Spectrom.* **1999**, *193*, 143–152.
(26) Wyttenbach, T.; Von Helden, G.; Bowers, M. T. *Int. J. Mass Spectrom. Ion Proc.* **1997**, *165/166*, 377–390.
(27) Julian, R. R.; Beauchamp, J. L. *Int. J. Mass Spectrom.* **2001**, *210/211*, 613–623.
(28) Ly, T.; Julian, R. R. *J. Am. Soc. Mass Spectrom.* **2006**, *17*, 1209–1215.
(29) Jensen, J. H.; Gordon, M. S. *J. Am. Chem. Soc.* **1995**, *117*, 8159–8170.
(30) Xu, S.; Nilles, J. M.; Bowen, J. K. H. *J. Chem. Phys.* **2003**, *119*, 10696–10701.
(31) Bush, M. F.; O'Brien, J. T.; Prell, J. S.; Saykally, R. J.; Williams, E. R. *J. Am. Chem. Soc.* **2007**, *129*, 1612–1622.
(32) Lebrilla, C. B. *Acc. Chem. Res.* **2001**, *34*, 653–661.
(33) Ramirez, J.; Ahn, S. H.; Grigorean, G.; Lebrilla, C. B. *J. Am. Chem. Soc.* **2000**, *122*, 6884–6890.
(34) Ahn, S. H.; Cong, X.; Lebrilla, C. B.; Gronert, S. *J. Am. Soc. Mass Spectrom.* **2005**, *16*, 166–175.
(35) Zhang, H.; Paulsen, E. S.; Walker, K. A.; Krakowiak, K. E.; Dearden, D. V. *J. Am. Chem. Soc.* **2003**, *125*, 9284–9285.
(36) Senko, M. W.; Canterbury, J. D.; Guan, S.; Marshall, A. G. *Rapid Commun. Mass Spectrom.* **1996**, *10*, 1839–1844.
(37) Wigger, M.; Nawrocki, J. P.; Watson, C. H.; Eyler, J. R.; Benner, S. A. *Rapid Commun. Mass Spectrom.* **1997**, *11*, 1749–1752.
(38) Chen, L.; Wang, T.-C. L.; Ricca, T. L.; Marshall, A. G. *Anal. Chem.* **1987**, *59*, 449–454.
(39) Gauthier, J. W.; Trautman, T. R.; Jacobson, D. B. *Anal. Chim. Acta* **1991**, *246*, 211–225.
(40) Jiao, C. Q.; Ranatunga, D. R. A.; Vaughn, W. E.; Freiser, B. S. *J. Am. Soc. Mass Spectrom.* **1996**, *7*, 118–122.
(41) Wyttenbach, T.; Kemper, P. R.; Bowers, M. T. *Int. J. Mass Spectrom.* **2001**, *212*, 13–23.
(42) Clemmer, D. E.; Jarrold, M. F. *J. Mass Spectrom.* **1997**, *32*, 577–592.
(43) Bowers, M. T.; Kemper, P. R.; von Helden, G.; van Koppen, P. A. M. *Science* **1993**, *260*, 1446–1451.
(44) von Helden, G.; Hsu, M.-T.; Kemper, P. R.; Bowers, M. T. *J. Chem. Phys.* **1991**, *95*, 3835–3837.
(45) Wyttenbach, T.; Bowers, M. T. *Top. Curr. Chem.* **2003**, *225*, 207–232.
(46) Mason, E. A.; McDaniel, E. W. *Transport Properties of Ions in Gases*; Wiley: New York, 1988.
(47) Case, D. A.; Pearlman, D. A.; Caldwell, J. W.; Cheatham, T. E. I.; Wang, J.; Ross, W. S.; Simmerling, C. L.; Darden, T. A.; Merz, K. M.; Stanton, R. V.; Cheng, A. L.; Vincent, J. J.; Crowley, M.; Tsui, V.; Gohlke, H.; Radmer, R. J.; Duan, Y.; Pitera, J.; Massova, I.; Seibel, G. L.; Singh, U. C.; Weiner, P. K.; Kollman, P. A. *AMBER 7*, University of California: San Francisco, CA, 2002.
(48) Wyttenbach, T.; von Helden, G.; Batka, J. J., Jr.; Carlat, D.; Bowers, M. T. *J. Am. Soc. Mass Spectrom.* **1997**, *8*, 275–282.
(49) Halgren, T. A. *J. Comput. Chem.* **1996**, *17*, 490–519.
(50) Apra, E.; Windus, T. L.; Straatsma, T. P.; Bylaska, E. J.; de Jong, W.; Hirata, S.; Valiev, M.; Hackler, M. T.; Pollack, L.; Kowalski, K.; Harrison, R. J.; Dupuis, M.; Smith, D. M. A.; Nieplocha, J.; Tipparaju, V.; Krishnan, M.; Auer, A. A.; Brown, E.; Cisneros, G.; Fann, G. I.; Fruchtl, H.; Garza, J.; Hirao, K.; Kendall, R.; Nichols, J. A.; Tsemekhman, K.; Wolinski, K.; Anchell, J.; Bernholdt, D.; Borowski, P.; Clark, T.; Clerc, D.; Dachsel, H.; Deegan, M.; Dyall, K.; Elwood, D.; Glendening, E.; Gutowski, M.; Hess, A.; Jaffe, J.; Johnson, B.; Ju, J.; Kobayashi, R.; Kutteh, R.; Lin, Z.; Littlefield, R.; Long, X.; Meng, B.; Nakajima, T.; Niu, S.; Rosing, M.; Sandrone, G.; Stave, M.; Taylor, H.; Thomas, G.; van Lenthe, J.; Wong, A.; Zhang, Z. *NWChem, A Computational Chemistry Package for Parallel Computers*; Pacific Northwest National Laboratory: Richland, WA, 2005.
(51) Humphrey, W.; Dalke, A.; Schulten, K. *J. Mol. Graphics* **1996**, *14*, 33–38.
(52) Oh, K. S.; Yoon, J.; Kim, K. S. *J. Phys. Chem. B* **2001**, *105*, 9726–9731.
(53) Bernstein, S. L.; Wyttenbach, T.; Baumketner, A.; Shea, J. E.; Bitan, G.; Teplow, D. B.; Bowers, M. T. *J. Am. Chem. Soc.* **2005**, *127*, 2075–2084.
(54) Roepstorff, P.; Fohlman, J. *Biomed. Mass Spectrom.* **1984**, *11*, 601.
(55) Zhang, H.; Ferrell, T. A.; Asplund, M. C.; Dearden, D. V. *Int. J. Mass Spectrom.* **2007**, *265*, 187–196.
(56) Breuker, K.; Oh, H; Lin, C.; Carpenter, B. K.; McLafferty, F. W. *Proc. Natl. Acad. Sci. U.S.A.* **2004**, *101*, 14011–14016.
(57) Oh, H.; Breuker, K.; Sze, S. K.; Ge, Y.; Carpenter, B. K; McLafferty, F. W. *Proc. Natl. Acad. Sci. U.S.A.* **2002**, *99*, 15863–15868.
(58) McLafferty, F. W.; Horn, D. M.; Breuker, K.; Ge, Y.; Lewis, M. A.; Cerda, B.; Zubarev, R. A.; Carpenter, B. K. *J. Am. Soc. Mass Spectrom.* **2001**, *12*, 245–249.
(59) Ackermann, B. L.; Barbuch, R. J.; Coutant, J. E.; Krstenansky, J. L.; Owen, T. J. *Rapid Commun. Mass Spectrom.* **1992**, *6*, 257–264.

JP808625V